Architecture of Star−Block Copolymers Consisting of Triblock Arms via a *N,N*-Diethyldithiocarbamate-Mediated Living Radical Photo-Polymerization and Application for Nanocomposites by Using as Fillers

Koji Ishizu* and Koichiro Ochi

Department of Organic Materials and Macromolecules, International Research Center of Macromolecular Science, Tokyo Institute of Technology, 2-12-1-H-133, Ookayama, Meguro-ku, Tokyo 152-8552, Japan

Received January 9, 2006; Revised Manuscript Received March 15, 2006

ABSTRACT: Highly branched poly(methyl methacrylate) (PMMA) stars were prepared by one-pot approach based on *N,N*-diethyldithiocarbamate- (DC-) mediated living radical photopolymerization. Soluble alternating hyperbranched microgel formation was initiated fast with preferential consumption of inimer 4-vinylbenzyl *N,N*-diethyldithiocarbamate (VBDC) and 4,4′-bismaleimidediphenylmethane (BMIM) in the presence of an excess of methyl methacrylate (MMA). PMMA arms could then grow from DC groups of microgel as macroinitiator. Next, star−block copolymers consisting of diblock arms [$(AB)_f$-DC; arm: PMMA-*block*-poly(*n*-butyl methacrylate) (PBMM)] were synthesized by photoinduced atom transfer radical polymerization (ATRP) of *n*-butyl methacrylate (BMM) initiated by the functionalized PMMA star $(A)_f$-DC in the presence of CuCl/bipyridine (bpy) catalyst. Subsequently, star−block copolymers consisting of triblock arms [$(ABA)_f$-DC; arm = PMMA-*block*-PBMM-*block*-PMMA] were synthesized by similar method initiated by $(AB)_f$-DC macroinitiator. It was found from light scattering data that such $(AB)_f$ and $(ABA)_f$ star−block copolymers (arm number $f = 28$) not only took spherical shape but also formed a single molecule in solution. We performed the construction of nanocomposites by using these $(ABA)_f$ stars as fillers. Free radical polymerization products from the mixture of MMA and $(ABA)_f$ star provided transparent fims. It was found from electron microscopy observations that $(ABA)_f$ stars distributed molecularly and homogeneously in a PMMA matrix, because such star−block copolymers promoted the ordering strucrure.

Introduction

Star polymers are of interest because they have an elementary branching topology, with multiple linear chains linked to a single core. In general, strategies toward making well-defined star polymers follow one of the two routes. In the "arm-first" approach, monofunctional linear polymers are first synthesized by living polymerization and then coupled to multifunctional cross-linking agents to form the star molecules. In the "core-first" approach, multifunctional initiators are used to grow arms by living polymerization. Recently, we presented a versatile, one-pot approach to highly branched stars on *N,N*-diethyldithiocarbamate (DC)-mediated living radical photo- polymerization.[1] In this approach, 4-vinylbenzyl diethyldithiocarbamate (VBDC), 4,4′-bismaleimidediphenylmethane (BMIM), and methyl methacrylate (MMA) were employed. VBDC acted as an inimer and BMIM was a cross-linking agent. The key to such star synthesis was the possibility of initial microgelation formation by the preferential and controlled alternating copolymerization of VBDC with bismaleimide derivatives. As a result, soluble alternating hyperbranched microgel formation was initially fast with preferential consumption of inimer VBDC and BMIM due to high propagation rate constant. Poly(methyl methacrylate) (PMMA) arm could then grow from DC groups of microgel core as macroinitiator (see Scheme 1). The styrene/maleimide alternating copolymer was formed with the exclusion of MMA incorporation into the chain. Hawker et al.[2] reported the synthesis of unusual block copolymers by copolymerization of styrene/maleic anhydride mixtures using nitroxide-mediated living radical polymerization. When an excess of styrene was used, the copolymerization led to preferential and finally total consumption of maleic anhydride at conversion of styrene significantly less than 100% due to high propagation of alternating polymerization. This result also supports the initial hyperbranched microgel formation by alternating copolymerization of VBDC and BMIM. Deng et al.[3,4] also reported star polystyrene (PS) in one-pot by copolymerization of bismaleimide derivaties with an excess of styrene under atom transfer radical polymerization (ATRP). This idea is the almost same as our strategies for the star synthesis. On the other hand, Li and Qui[5] have made clear that reverse ATRP with a benzoyl peroxide (BPO) initiator can be catalyzed by a copper(II) compound, Cu(DC)Cl. The polymerization of MMA initiated by BPO/Cu(DC)Cl/bipyridine (bpy) was successfully performed in a living fashion. On the basis of the above experimental results, it can be speculated that iniferters will be utilized for photoinduced ATRP. To prove the living fashion of photoinduced ATRP, bulk photopolymerization of *t*-butyl methacrylate (BMA) were carried out initiated by benzyl *N,N*-diethyldithiocarbamate (BDC; as a model compound), varying the UV irradiation time in the presence of CuCl/bpy catalysis.[6] It was found from kinetic analysis that photoinduced ATRP proceeded with living radical mechanism. In this polymerization a copper complex, Cu(DC)Cl/bpy reversibly activated the dormant polymer chains via a DC transfer reaction such as Cu(DC)Cl/bpy, and it was dynamic equilibrium that was responsible for the controlled behavior of the polymerization of BMA.

* To whom correspondence should be addressed. E-mail: kishizu@polymer.titech.ac.jp.

10.1021/ma0600512 CCC: $33.50
Published on Web 04/07/2006

Scheme 1. Reaction Scheme for $(ABA)_f$ Star−Block Copolymer Synthesis

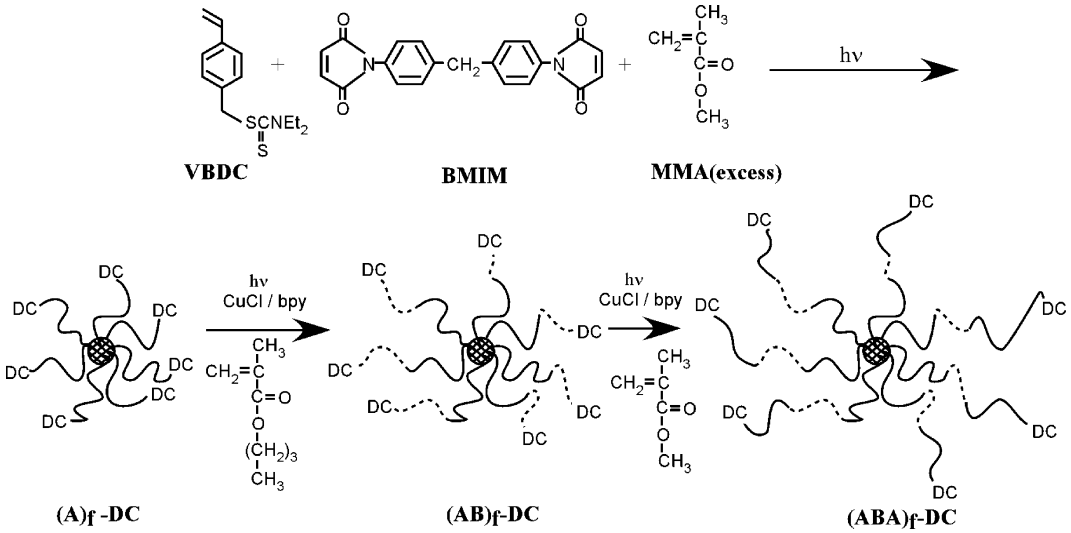

The interest in star polymers arises not only from the fact that they are models for branched polymers but also from their enhanced segment densities. We investigated in detail the structural ordering of typical two types of stars by means of small-angle X-ray scattering (SAXS).[7,8] Polyisoprene (PI) stars (arm number $f >$ ca. 90) formed a body-centered-cubic (bcc) structure near the overlap threshold (C^*). Moreover, polyelectrolyte stars poly(*tert*-butyl acrylate)s (with high functionality $f = 30$ and 97) also formed a bcc structure in aqueous solution of near the C*.[9,10] Even polyelectrolyte star with low arms ($f = 30$) showed regular ordering due to electrostatic double layers.

The star−block copolymers have a molecular conformation similar to star polymers. De la Cruz and Sanchez[11] have calculated the phase-stability criteria and static structure factors in the weak-segregation limits for an *f*-arm diblock copolymer [$(AB)_f$ star]. According to their results, as the *f* becomes large, the $(AB)_f$ star begins to develop a "core and shell"-type structure. Their self-segregation or self-micellization tends to create significant concentration fluctuations at the core−shell interface. Then, we prepared the $(AB)_f$ stars ($f = 14-41$ and 16−19 wt % PI blocks) by anionic copolymerization of PS-*block*-PI diblock anions with divinylbenzene (DVB).[12] This $(AB)_f$ star ($f = 16$) formed a bcc structure near the C^* and such structure changed to a face-centered-cubic (fcc) lattice in the bulk film.[12,13] The structural ordering of $(AB)_f$ star copolymers was very similar to that observed on the star polymers.

On the other hand, polymer-based nanocomposites may offer a significant improvement in many physical and engineering properties with a very low filler loading. Among these properties are stiffness, strength, dimensional stability, and permeability.[14−18] There has been considerable interest in developing filled systems where the polymeric component is a star-shaped polymer. In principle, the star−block copolymers promote the ordering of the particles and thereby create highly organized hybrid materials.

We can expect the architecture of multicomponent star−block copolymers by grafting on functionalized stars as macroinitiator with various vinyl monomers, because the stars obtained in one-pot polymerization[1] have a photofunctional DC group at each arm end. Herein, star−block copolymers consisting of triblock arms [arm = PMMA-*block*-poly(*n*-butyl methacrylate) (PBMM)-*block*-PMMA] were synthesized by a combination of free radical processes: (1) alternating copolymerization, (2) photo-DC controlled radical polymerization, and (3) ATRP. We studied their dilute-solution properties by means of static and dynamic light scatterings (SLS and DLS) and solid properties from transmission electron (TEM) and atomic force microscopy (AFM) observations. We also constructed the nanocomposites by free radical polymerization of MMA containing $(ABA)_f$ star particles as fillers.

Experimental Section

Materials. The functionalized PMMA stars were prepared by living radical polymerization of a 100:2:2 equiv mixture of MMA, inimer VBDC (Nissan Chemical Industries, Ltd., Tokyo), and BMIM (Tokyo Kasei Organic Chemicals, Tokyo) in tetrahydrofuran (THF; 50% solution) under UV irradiation (1 h). Details concerning the synthesis and purification have been given elsewhere.[1] MMA and *n*-butyl methacrylate (BMM: Tokyo Kasei Organic Chemicals, Tokyo) were distilled under high vacuum. Toluene, THF, methanol, CuCl, and bpy (Tokyo Kasei Organic Chemicals, Tokyo), 2,2′-azobis(4- methoxy-2,4-dimethylvaleronitrile) (V-70; 10 h half-life decomposition temperature 30 °C; Wako Pure Chemical Industries, Ltd., Tokyo), I_2 (Kanto Kagaku Reagent Division, Tokyo), and RuO_4 (Rare Metalic, Tokyo) were used as received.

Synthesis of Star—Block Copolymers Consisting of Triblock Arms. The synthesis route for star−block copolymers consisting of triblock arms $(ABA)_f$ is outlined in Scheme 1.

DC-mediated polymerization operations were carried out in a sealed glass ampule at 30 °C under the UV irradiation (250 W high-pressure mercury lamp, Ushio Denki SX-UI 250 HAMQ, Tokyo; UV intensity 42 mW/cm^2, irradiation distance 15 cm). First, $(AB)_f$ stars (arm: PMMA-*block*-PBMM) was synthesized by photoinduced ATRP of BA initiated by the functionalized PMMA star $(A)_f$-DC in toluene under the condition [$(A)_f$-DC]: [BMM]: [CuCl]:[bpy] = 1:1000:1.2:2.5, where [$(A)_f$-DC] indicates DC concentration of PMMA star; 10−25 h of UV irradiation time. After polymerization, the polymer was recovered by precipitation in methanol. Subsequently, $(ABA)_f$ stars were synthesized by similar method in toluene under the condition [$(AB)_f$-DC]:[MMA]: [CuCl]: [bpy] = 1:1000:1.2:2.5; 15 h of UV irradiation time. The $(ABA)_f$ star was also recovered by precipitation in methanol. The conversion was estimated by gravimetric measurements.

Construction of Nanocomposites. The prescribed MMA solution of $(ABA)_f$-DC stars was poured into a Petri dish. Free radical polymerization of MMA was carried out in the presence of V-70 (3 wt % for monomer) in nitrogen atmosphere at 30 °C for 24 h.

Characterization. The molecular weight distributions (M_w/M_n) of star and star−block copolymers were determined by gel permeation chromatography (GPC; Tosoh high-speed liquid chromatograph HLC-8120, Tokyo) using two TSK gel columns, GMH_{XL}

[excluded-limit molecular weight ($M_{ELM} = 4 \times 10^8$)] and G2000H_{XL} ($M_{ELM} = 1 \times 10^4$), in series in THF as eluent (flow rate of 1.0 mL/min) at 40 °C using PMMA standard samples. The weight-average molecular weights (M_w) of star and star−block copolymers were determined by SLS (Photal TMLS-6000HL: Otsuka Electronics, Tokyo; He−Ne laser: $\lambda_0 = 632.8$ nm) using Zimm mode in THF ($n_D = 1.40$, $\eta = 0.456$ cP) at 25 °C. The refractive index increment dn/dc of each star or star−block copolymer was determined by differential refractometer (Photal DRM-1021). Sample solutions were filtered through membrane filters with a nominal pore of 0.2 μm just before measurement. The scattering angle was in the range 30−150°.

The hydrodynamic radius (R_h) of star and star−block copolymers was evaluated using Stokes−Einstein equation from the diffusion coefficient (D_0) determined by DLS (Otsuka Electronics) data with cumulant method in THF at 25 °C (scattering angle of 90°).

The formations of star−block copolymer $(AB)_f$ and $(ABA)_f$ were recognized by ^{1}H NMR (500 MHz, JEOL GSX-500 NMR spectrometer, Tokyo) in $CDCl_3$ (methoxy protons (δ 3.62 ppm) of PMMA, methyl protons (1.48 ppm) of *n*-butyl groups of PBA and ethylene protons (3.99 ppm) of *n*-butyl groups adjacent to ester bond).

AFM photographs were recorded with a JSPM-4210 scanning probe microscope (JEOL, Tokyo) operating in the tapping mode. The measurements were perfomed in air using Si cantilevers with a spring constant of 0.65 N/m, a tip radius of 10 nm, and a resonance frequency of 40 kHz. The samples for tapping mode AFM measurements were prepared by spin-casting on a rotating mica substrate at 2000 rpm of dilute solutions of $(A)_f$, $(AB)_f$, and $(ABA)_f$ stars in THF.

Morphological observations for $(A)_f$, $(AB)_f$, and $(ABA)_f$ stars were performed by TEM (JEOL JEM-200CX, Tokyo) at an accelerating voltage of 75 kV. The specimens were prepared by placing 0.1 wt % THF solutions of star and star−block copolymers on copper grids coated with a thin carbon film and stained with I_2 vapor. This reagent stained selectively with both PMMA and PBMM domains. For two-dimensional observation of the packing structure of the $(ABA)_f$ stars in nanocomposites, an ultrathin film 80 nm thick was prepared by cutting with a microtome (Reinhert-Nissei Co., Ultracut N) and stained with RuO_4. This reagent stained selectively with DC groups.[19]

Differential scanning calorimetry (DSC) measurements were recorded on a Seiko Instrument (DSC 220C, Tokyo) to determine glass transition temperature (T_g) of nanocomposites. Indium and zinc were used as calibration standards. Heating rate was 10 °C/min.

Dynamic mechanical analysis (DMA) was performed in an ARES rheometer (Rheometric Scientific). Frequency dependencies of the complex shear modulus at a reference temperature (master curves) were determined from frequency sweeps measured with a small-amplitude, sinusoidal deformation at various temperatures under a dry nitrogen atmosphere. Temperature dependencies at a constant deformation rate were measured independently.

Results and Discussion

Synthesis and Characterization of $(ABA)_f$ Stars. PMMA star $(A)_f$-DC was synthesized by living radical polymerization of a mixture of MMA, inimer VBDC and BMIM in THF, conformed to previous work[1] (yield 48% from gravimetric measurement).

A typical GPC profile of $(A_{40})_{28}$-DC is shown in Figure 1 using RI detector. The GPC distribution has a single and relatively broad polydispersity ($M_w/M_n = 2.1$). The M_w (3.98×10^5) was determined by SLS with Zimm mode in THF. To elucidate the arm number f of the star molecule, we determined the content of DC groups by ^{1}H NMR spectrum in $CDCl_3$. Figure 2a shows a typical ^{1}H NMR spectrum of $(A_{40})_{28}$-DC star. The broad peaks observed at δ 6.9−7.4 ppm (d, i) are attributed to the phenyl groups of VBDC and BMIM units. A strong peak at 3.62 ppm (c) is assignable to the methoxy protons

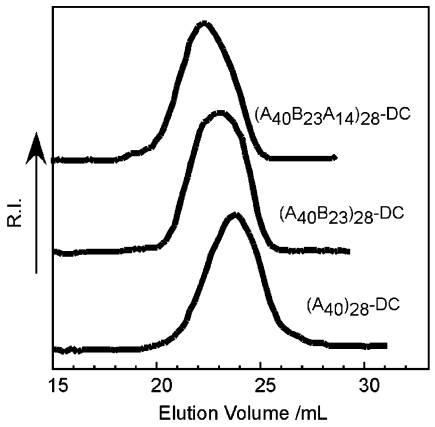

Figure 1. GPC profiles of stars $(A_{40})_{28}$-DC, $(A_{40}B_{23})_{28}$-DC, and $(A_{40}B_{23}A_{14})_{28}$-DC. GPC measurements were carried out in THF at 40 °C.

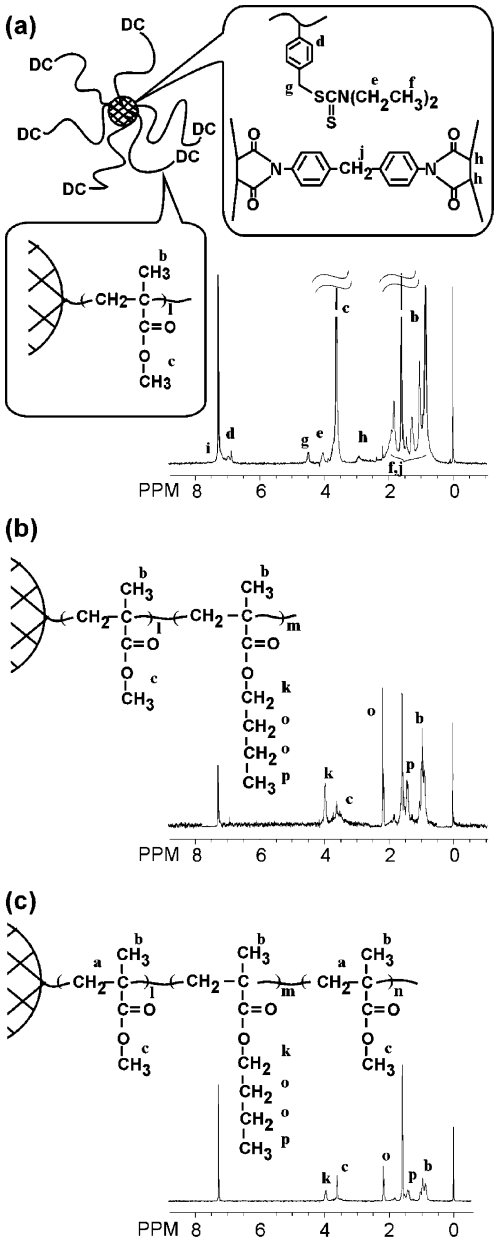

Figure 2. ^{1}H NMR spectra of stars $(A_{40})_{28}$-DC (a), $(A_{40}B_{23})_{28}$-DC (b), and $(A_{40}B_{23}A_{14})_{28}$-DC (c) in $CDCl_3$.

Table 1. Polymerization Conditions and Results of Star-Shaped Polymers[a]

	polymerization conditions		star-shaped polymers				
code	irradiation time (h)	monomer concn (%)	convn (%)	$10^{-5}M_w$[b]	M_w/M_n[c]	R_h[d] (nm)	DP_n (arm block)
$(A_{40})_{28}$-DC	1	50	48	3.98	2.1	3.2	40 (PMMA)[f]
$(A_{40}B_{10})_{28}$-DC[e]	10	40	5	4.39	1.6	7.4	10 (PBMM)[g]
$(A_{40}B_{10}A_{89})_{28}$-DC[e]	15	50	4	8.65	1.5	9.6	89 (PMMA)[g]
$(A_{40}B_{23})_{28}$-DC[e]	10	50	10	5.06	1.8	4.6	23 (PBMM)[g]
$(A_{40}B_{23}A_{14})_{28}$-DC[e]	15	50	2	5.43	1.7	9.7	14 (PMMA)[g]
$(A_{40}B_{188})_{28}$-DC[e]	25	50	7	22.3	2.4	20.6	188 (PBMM)[g]
$(A_{40}B_{188}A_{125})_{28}$-DC[e]	15	50	2	30.7	2.4	26.6	125 (PMMA)[g]

[a] Arm number $f = 28$. [b] Determined by SLS with Zimm mode in THF at 25 °C. [c] Determined by GPC profiles using PMMA standard samples. [d] Determined by DLS in THF at 25 °C. [e] Polymerized by photoinduced ATRP; [DC]:[M]:[CuCl]:[bpy] = 1:1000:1.2:2.5, where [M] indicates BMM or MMA monomer concentration. [f] Estimated by ^{1}H NMR spectrum and M_w. [g] Estimated by f and M_w, assuming that arm chains are generated from all the DC groups of macroinitiators.

of PMMA. The small peak at 4.0 ppm (e) is assignable to the methylene protons of DC groups. The molar ratio of the DC unit to MMA unit in this star was determined as 1:68 from the signal intensity ratio of methylene groups (e; 4.0 ppm) to the methoxy groups (c; 3.62 ppm). We calculated the arm number using the weight-average molecular weight, because this star was not monodisperse sample. Therefore, the arm number was calculated to be 28, i.e., $3.98 \times 10^5/2.1/100/68 = 28$. These characteristics are listed in Table 1.

On the other hand, Sigwalt et al.[20−22] and Turner et al.[23] reported the mechanism of polymerization of *n*-butyl acrylate and block copolymer formation using DC free-radical chemistry. They proposed a photochemical cleavage of the thiocarbonyl-nitrogen bond and subsequent elimination of CS_2 as the decomposition pathway. In this work, such side reactions do not seem to take place during polymerization, regardless of relatively broad polydispersity. These problems will be mentioned in the section on star−block copolymer synthesis.

In preliminary experiment, "grafting from" polymerization of monomer BMM initiated by PMMA star initiator $(A_{40})_{28}$-DC under UV irradiation led often to macrogelation due to intermolecular radical couplings. The main reasons are the following two: (1) high localized radical concentration on the star surface and (2) high propagation rate of PBMM radicals. Then, we employed photoinduced ATRP for such "grafting from" process. $(AB)_f$-DC stars (arm: PMMA-*block*-PBMM) were synthesized by photoinduced ATRP of BMM monomer initiated by $(A_{40})_{28}$-DC as a macroinitiator in toluene, varying the monomer concentration and UV irradiation time. Polymerization conditions and results are listed in Table 1. A typical GPC profile of $(A_{40}B_{23})_{28}$-DC is also shown in Figure 1. The GPC distribution has a single pattern and shifts to high-molecular-weight side compared to that of $(A_{40})_{28}$-DC precursor. The polydispersity ($M_w/M_n = 1.8$) becomes somewhat narrower than that of $(A_{40})_{28}$-DC precursor due to high enhanced segment density. The propagation rate of BMM with the addition of CuCl/bpy was very slow compared to that without CuCl/bpy, under similar conditions. This means that the dynamic equilibrium with CuCl/bpy is faster than without CuCl/bpy system. So, the system with CuCl/bpy assists to the controlled living radical polymerization compared to without CuCl/bpy system. These results support good functionality of PMMA star initiator, that is, PMMA arm exhibited a DC group at its terminal end. More recently, Zhang et al.[24] have reported ATRP of styrene using the initiator ethyl 2-*N*,*N*-(diethylamino)dithiocarbamoyl-butylate. The results of ^{1}H NMR analysis and chain extension demonstrated that well-defined PS bearing a photolabile group was synthesized via ATRP, and almost no exchange occurred between the DC group and the halogen atoms in the catalyst. This result was different from the reports by Li and Qui[5] and our works. The mechanism for photoinduced ATRP involves some problems to be solved.

A typical ^{1}H NMR spectrum of $(A_{40}B_{23})_{28}$-DC in $CDCl_3$ is shown in Figure 2b. This spectrum indicates the expected resonances for the methyl protons (p: 1.48 ppm) of *n*-butyl groups and the ethylene protons (k: 3.99 ppm) of *n*-butyl groups adjacent to ester bond. However, the peak intensity of methoxy protons (c: around 3.7 ppm) of internal PMMA blocks decreases as compared with that of $(A_{40})_{28}$-DC. Moreover, the phenyl protons of microgel core disappear completely due to small mass or slow relaxation. This result indicates clearly that not only the microgel core but also internal PMMA block segments contribute a micellar core which behaves as a solid on the time scale of segment relaxation. The degree of polymerization (DP_n) of PBMM blocks was estimated to be 23 from the arm number and molecular weight determined by SLS, assuming that PBMM polymer chains are generated from all the DC groups of $(A_{40})_{28}$-DC macroinitiator. These characteristics are also listed in Table 1.

Subsequently, $(ABA)_f$-DC stars were also synthesized by photoinduced ATRP of MMA initiated by $(AB)_f$-DC as a macroinitiator in toluene (see the polymerization conditions and results in Table 1). A typical GPC profile of $(A_{40}B_{23}A_{14})_{28}$-DC is also shown in Figure 1. The GPC distribution has a single pattern and shifts to high-molecular-weight side compared to that of $(A_{40}B_{23})_{28}$-DC precursor. The polydispersity ($M_w/M_n = 1.7$) was almost the same as $(A_{40}B_{23})_{28}$-DC ($M_w/M_n = 1.8$). A typical ^{1}H NMR spectrum of $(A_{40}B_{23}A_{14})_{28}$-DC is shown in Figure 2c. It is found from this spectrum that the methoxy protons (c: 3.66 ppm) of external PMMA block have stronger intensity than the ethylene protons (k: 3.99 ppm) of *n*-butyl groups adjacent to ester bond for middle PBMM blocks. The DP_n of external PMMA blocks was estimated to be 14 from the arm number and the molecular weight determined by SLS. The conversions of $(AB)_f$-DC and $(ABA)_f$-DC stars were less than 10%.

Solution and Solid Properties of Star and Star—Block Copolymers. To discuss the geometrical anisotropy and intermolecular interaction, we determined the translational diffusion coefficient $D(C)$ of $(AB)_f$-DC and $(ABA)_f$-DC stars. In general, the mutual diffusion coefficient $D(C)$ is defined as $D(C) \equiv \Gamma_e q^{-2}{}_{\theta\to 0}$, where θ and Γ_e are the scattering angle and the first cummulant, respectively. The angular dependence of $\Gamma_e q^{-2}$ ($qR_h < 1$) for $(A_{40}B_{23})_{28}$-DC and $(A_{40}B_{23}A_{14})_{28}$-DC is shown in Figure 3.

In the case of a spherical shape, it is well-known that the slope of the line ($\Gamma_e q^{-2}$ vs q^2) is zero. Both sets of observed data of star−block copolymers almost fitted on a flat line. Therefore, it seems that both star−block copolymers take the shape of a sphere in dilute solution.

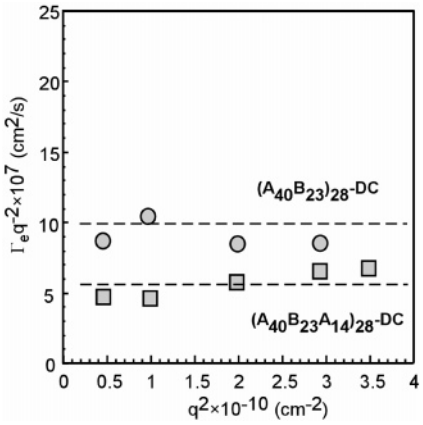

Figure 3. Angular dependence $\Gamma_e q^{-2}$ vs q^2 for $(A_{40}B_{23})_{28}$-DC and $(A_{40}B_{23}A_{14})$-DC stars in THF at 25 °C.

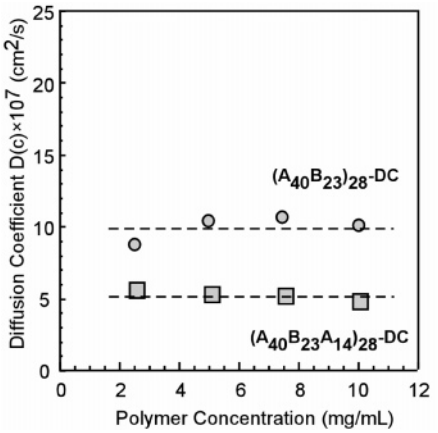

Figure 4. Plots of diffusion coefficient $D(C)$ against polymer concentration C for $(A_{40}B_{23})_{28}$-DC and $(A_{40}B_{23}A_{14})_{28}$-DC stars in THF at 25 °C.

Figure 4 shows the relationship between the translational diffusion coefficient $D(C)$ and the polymer concentration C for $(A_{40}B_{23})_{28}$-DC and $(A_{40}B_{23}A_{14})_{28}$-DC stars (scattering angle 90°). Each $D(C)$ has a constant value in the range 0−10 mg/mL polymer concentration for all the samples. This suggests that these star−block copolymers form a single molecule at such polymer concentrations. The segment density of star-shaped polymers is very high, even in a good solvent, due to the compact structure. The translational diffusion coefficient D_0 can be estimated by extrapolation of the polymer concentration C to zero. R_h is defined as the Stokes−Einstein equation: $R_h = kT/6\pi\eta_0 D_0$, where k, T, and η_0 are the Boltzmann coefficient, the absolute temperature, and the viscosity of the solvent, respectively. The values of R_h are also listed in Table 1.

Figure 5 shows the size distributions on DLS data of $(A_{40})_{28}$-DC, $(A_{40}B_{188})_{28}$-DC, and $(A_{40}B_{188}A_{125})_{28}$-DC stars in THF. All the profiles show unimodal distributions and after grafting of BMM and MMA monomers the hydrodynamic diameter (D_h) increases to 41.2 and 53.2 nm in the order compared to that (D_h = 6.4 nm) of $(A_{40})_{28}$-DC star. It is concluded from the above results that star−block copolymers form a single molecule with spherical shape even in a good solvent. In other words, such star−block copolymers behave as nanospheres in solution, regardless of there being no cross-linked structure.

Typical AFM photographs of $(A_{40})_{28}$-DC and $(A_{40}B_{188}A_{125})_{28}$-DC are shown in Figure 6, parts a and b, respectively. Spherical particles are clearly visible for both samples. A ststistical analysis of the AFM image shows that the diameter and height of particles are 16 and 4.6 nm for $(A_{40})_{28}$-DC, and ca. 45 and

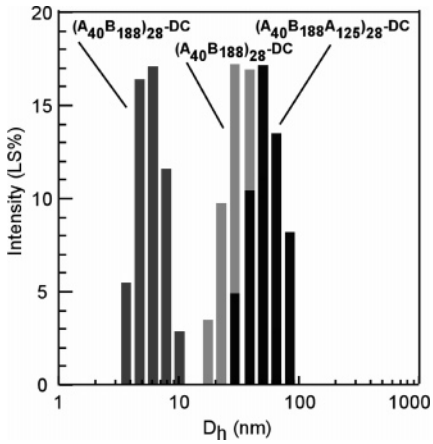

Figure 5. Size distribution on DLS data of $(A_{40})_{28}$-DC, $(A_{40}B_{23})_{28}$-DC, and $(A_{40}B_{23}A_{14})_{28}$-DC stars in THF at 25 °C.

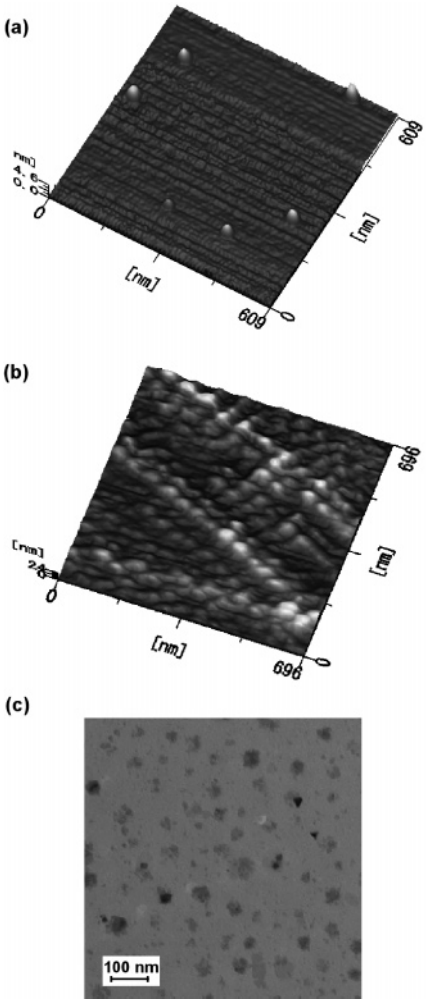

Figure 6. AFM photographs (side view) of stars $(A_{40})_{28}$-DC (a) and $(A_{40}B_{188}A_{125})_{28}$-DC (b) and a TEM photograph of $(A_{40}B_{188}A_{125})_{28}$-DC (c) stained with I_2.

24 nm for $(A_{40}B_{188}A_{125})_{28}$-DC, respectively. Figure 6a indicates a collapsed structure on the surface for PMMA star. On the other hand, Figure 6b indicates somewhat regular packing structure of $(ABA)_f$-DC stars. The diameter measured may be overestimated, because we used a trip radius of 10 nm for Si cantilever. Figure 6c shows TEM photograph of $(A_{40}B_{188}A_{125})_{28}$-DC. The dark and white portions correspond to $(ABA)_f$ star and carbon substrate, respectively. The particle diameter is ca. 40−50 nm. This result supports the data on AFM image.

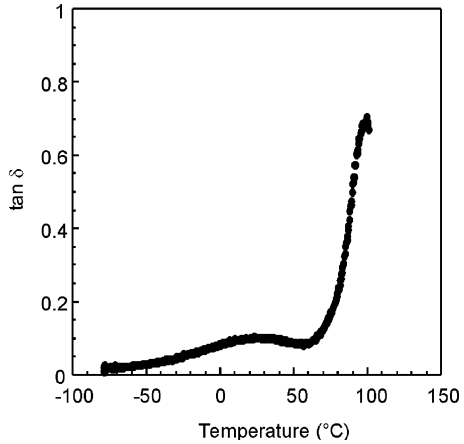

Figure 7. Temperature dependence of dynamic loss tangent (G''/G') (tan δ), where G' and G'' indicate the dynamic shear storage and loss moduli, respectively, for $(A_{40}B_{23}A_{14})_{28}$-DC star. Heating rate: 10 °C/min.

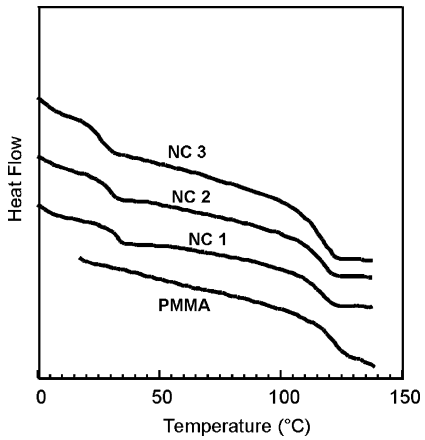

Figure 8. DSC traces for PMMA and nanocomposites NC1 [addition amount of $(A_{40}B_{10}A_{89})_{28}$-DC, 1 wt %], NC2 (5 wt %) and NC (10 wt %). Heating rate: 10 °C/min.

Figure 7 shows the temperature dependence of the dynamic loss tangent (G''/G') (tan δ), where G' and G'' indicate the dynamic shear storage and loss moduli (from −100 to +150 °C), respectively, for $(A_{40}B_{23}A_{14})_{28}$-DC star. This star shows two transitions in the vicinity of 20 and 100 °C, respectively, which are assigned to the glass transition of the PBMM and PMMA phases, respectively. This means that $(ABA)_f$-DC stars formed microphase-separated structure in the solid state. It can be expected from the above solution and solid properties that $(ABA)_f$ stars are promising materials as fillers, because such stars not only behave as nanospheres in solution but also exhibit microphase-separated structure.

Construction of Nanocomposites. Nanocomposites were prepared by free radical polymerization of MMA initiated by V-70, varying the addition amounts and the composition of $(ABA)_f$-DC stars. All the polymerization products provided transparent films. Measurement of the glass transition temperature (T_g) is the most rapid although not the most sensitive way to detect the phase separation in multicomponent polymer systems.

Figure 8 shows typical DSC traces for the nanocomposites NC1 [addition amount of $(A_{40}B_{10}A_{89})_{28}$-DC, 1 wt %], NC2 (5 wt %) and NC3 (10 wt %), varying the addition amounts of $(A_{40}B_{10}A_{89})_{28}$-DC stars. In all the cases, two T_g's are observed, which is a clear indication of phase separation, with the lowest T_g (T_{g1}) characteristic of the PBMM phase and the T_g at the higher temperature (T_{g2}) assigned to the PMMA phase. T_{g1} is diffuse due to the low content in PBMM. T_{g2} is essentially independent of the composite composition. On the other hand, DSC trace for PMMA corresponds to the sample polymerized with the same conditions in the absence of $(A_{40}B_{10}A_{89})_{28}$-DC stars. It is found that T_{g2} for nanocomposites somewhat decreases compared to T_g of PMMA. T_{g2} expectedly depends to the molecular weight of PMMA. The well-accepted reversible addition−fragmentation chain transfer (RAFT) mechanism is a chain transfer of propagating radical through the DC groups.[25] Then, the M_w of PMMA matrix of nanocomposites may be somewhat lower than that of PMMA, due to chain transfer of propagating radicals. However, the particle sizes were almost the same as original stars. The chain transfer reaction seems to occur with extremely small amounts.

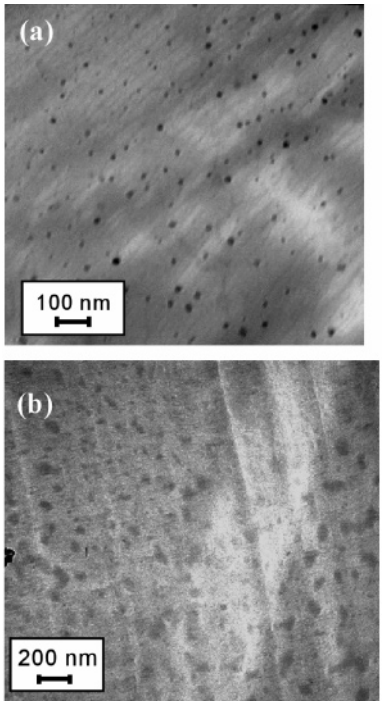

Figure 9. TEM photographs of nanocomposite film specimens stained with RuO_4: (a) NC2; (b) NC4 [addition amount of $(A_{40}B_{188}A_{125})_{28}$-DC, 20 wt %].

Figure 9 shows the TEM photographs of typical nanocomposites NC2 (a) and NC4 [addition amount of $(A_{40}B_{188}A_{125})_{28}$-DC, 20 wt %] (b), respectively. Dark portions correspond to $(ABA)_f$-DC stars. RuO_4 selectively stained DC groups on the nanosphere surfaces. On the other hand, white portions correspond to PMMA matrix. It is found from both photographs that MMA monomers form a continuous matrix phase around the $(ABA)_f$ nanospheres. Then, the $(ABA)_f$ stars are distributed molecularly in a PMMA matrix. As mentioned in the Introduction, star−block copolymers promote the ordering of the particles and moreover, the external PMMA block shells are miscible to PMMA matrix chains during free radical polymerization. Therefore, such stars can create highly organized hybrid materials. The $(ABA)_f$ stars are one of the most convenient fillers for the fabrication of nanocomposites.

Conclusions

Highly branched PMMA stars were prepared by one-pot synthesis based on DC-mediated living radical photopolymerization. These stars acted as macroinitiator, because the stars exhibited a DC group at each arm end. Subsequently, the well-defined $(ABA)_f$ star−block copolymers (arm: PMMA-*block*-PBMM-*block*-PMMA) were prepared stepwisely by "grafting

from" photoinduced ATRP techniques. These stars ($f = 28$) showed no angular dependence on DLS data in THF, and $D(C)$ had an almost constant value in the range 0−10 mg/mL polymer concentration. The $(ABA)_f$ stars formed a single molecule with spherical shape at such a polymer concentration. We constructed the nanocomposites by free radical polymerization of MMA using $(ABA)_f$ stars as fillers, varying the addition amount and the composition of $(ABA)_f$-DC stars. All the polymerization products provided transparent films and exhibited two T_g's assignable to PBMM and PMMA phases, which was a clear indication of phase separation. The TEM observations also indicated that such stars were distributed molecularly in a PMMA matrix. These star−block copolymers could create highly organized hybrid materials.

Supporting Information Available: Text giving the synthesis of PMMA star. This material is available free of charge via the Internet at http://pubs.acs.org.

References and Notes

(1) Ishizu, K.; Park, J.; Shibuya, T.; Sogabe, A. *Macromolecules* **2003**, *36*, 2990.
(2) Benoit, D.; Hawker, C. J.; Huang, E. E.; Lin, Z.; Russell, T. P. *Macromolecules* **2000**, *33*, 1505.
(3) Deng, G. H.; Chen, Y. M. *Macromolecules* **2004**, *37*, 18.
(4) Deng, G. H.; Cao, M.; Huang, J.; He, L.; Chen, Y. M. *Polymer* **2005**, *46*, 5698.
(5) Li, P.; Qiu, K. Y. *Macromol. Rapid Commun.* **2000**, *21*, 665.
(6) Ishizu, K.; Kakunuma, H. *J. Polym. Sci. Polym Chem. Ed.* **2005**, *43*, 63.
(7) Ishizu, K.; Ono, T.; Uchida, S. *J. Colloid Interface Sci.* **1997**, *192*, 189.
(8) Ishizu, K. In *Encyclopedia of Surface and Colloid Science*; Hubbard, A., Ed.; Marcel Dekker: New York, 2002, p 4862.
(9) Furukawa, T.; Ishizu, K. *Macromolecules* **2005**, *38*, 2911.
(10) Furukawa, T.; Ishizu, K. *Macromolecules* **2003**, *36*, 434.
(11) De la Cruz, M. O.; Sanchez, I. C. *Macromolecules* **1986**, *19*, 2501.
(12) Ishizu, K.; Uchida, S. *J. Colloid Interface Sci.* **1995**, *175*, 293.
(13) Ishizu, K.; Uchida, S. *Prog. Polym. Sci.* **1999**, *24*, 1439.
(14) Giannelis, E. P. *Adv. Mater.* **1996**, *8*, 29.
(15) Sherman, L. M. *Plast. Technol.* **1999**, *45*, 52.
(16) Ginzburg, V. V.; Singh, C.; Balazs, A. C. *Macromolecules* **2000**, *33*, 1089.
(17) Alexandre, M.; Dubois, P. *Mater. Sci. Eng.* **2000**, *28*, 1.
(18) Zanetti, M.; Lomakin, S.; Camino, G. *Macromol. Mater. Eng.* **2000**, *279*, 1.
(19) Staining effect of RuO_4 with DC groups was recognized by TEM observation of (styrene−VBDC) random copolymer.
(20) Lambrinos, P.; Tardi, M.; Polton, A.; Sigwalt, P. *Eur. Polym. Mater.* **1990**, *26*, 1125.
(21) Manga, J. D.; Polton, A.; Tardi, M.; Sigwalt, P. *Polym. Int.* **1998**, *45*, 14.
(22) Manga, J. D.; Tardi, M.; Polton, A.; Sigwalt, P. *Polym. Int.* **1998**, *45*, 243.
(23) Turner, S. R.; Blevins, R. W. *Macromolecules* **1990**, *23*, 1856.
(24) Zhang, W.; Zhu, X.; Zhu, J.; Chen, J. *J. Polym. Sci., Polym. Chem. Ed.* **2006**, *44*, 32.
(25) Chiefari, J.; Rizzardo, E. In *Handbook of Radical Polymerization*; Matyjaszewski, K., Davis, T. P., Eds.; Wiley-Interscience: Hoboken, NJ, 2002; p 629.

MA0600512